

See discussions, stats, and author profiles for this publication at: <https://www.researchgate.net/publication/231232541>

Two 3-D Cluster-Based Frameworks: Highly Eight-Connected Molecular Topology and Magnetism

ARTICLE *in* CRYSTAL GROWTH & DESIGN · JUNE 2009

Impact Factor: 4.89 · DOI: 10.1021/cg8013893

CITATIONS

58

READS

11

4 AUTHORS, INCLUDING:



Stuart R. Batten

Monash University (Australia)

311 PUBLICATIONS 14,406 CITATIONS

[SEE PROFILE](#)



Ji Zheng

Chinese Academy of Sciences

128 PUBLICATIONS 2,659 CITATIONS

[SEE PROFILE](#)

Two 3-D Cluster-Based Frameworks: Highly Eight-Connected Molecular Topology and Magnetism

Pang-kuan Chen,^{†,‡} Stuart R. Batten,[§] Yan Qi,[†] and Ji-Min Zheng^{*,†}

Department of Chemistry, Nankai University, Tianjin 300071, P. R. China, Department of Chemistry, Rutgers University, Newark, New Jersey 07102, and School of Chemistry, Monash University, Victoria 3800, Australia

Received December 21, 2008; Revised Manuscript Received March 17, 2009

ABSTRACT: A couple of metal-organic frameworks (MOFs) constructed from rigid bicarboxylates are presented herein, namely, $\text{Co}_3(\text{ndc})_3(\text{bbi})(\text{CH}_3\text{CN})_2$ (**1**) and $\text{Dy}_2\text{Mn}_3(\text{ndc})_6(\text{bipy})_2$ (**2**), where H_2ndc = 2,6-naphthalenedicarboxylic acid, bipy = 2,2'-pyridine, and bbi = 1,1'-(1,4-butanediyl)bis(imidazole). These two coordination polymers have been prepared through solvo/hydrothermal reactions and characterized by single-crystal X-ray study, TG, IR, and elemental analysis. Polymer **1** features a novel self-penetrating network mediated by flexible long-chain ligand and well defines a unique $4^{16}\cdot 5^8\cdot 6^4$ topology with the treatment of Co_3 unit as an 8-connected node, which equals the highest connectivity for monometallic self-penetrating system so far. Polymer **2** represents the first example of a $\text{Mn}^{\text{II}}\text{--Dy}^{\text{III}}$ (3d-4f) heteropentanuclear complex showing an intriguing 3-D $3^6\cdot 4^{18}\cdot 5^3\cdot 6$ framework upon the assignment of Dy_2Mn_3 cluster to an 8-connected node. In addition, magnetic studies of **1** reveal that the antiferromagnetic behavior is operative within the trimeric Co_3 cluster and **2** demonstrates dominant ferromagnetic coupling interactions between Dy^{III} and Mn^{II} ions.

Introduction

Construction and characterization of highly entangled network solids has attracted significant interest, not only due to their aesthetic appeal and interesting topologies¹ but also due to the potential applications of such materials.² Recently, there has been much progress in the discovery of entangled polymeric systems such as self-penetrating (self-catenating) networks, interpenetrating (polycatenating) networks, and rotaxanes. However, the majority of the reported entanglements fall into the interpenetrating category, as evidenced by several comprehensive reviews providing some insightful information on the rationalization and classification of their topologies.³ Unlike interpenetration, self-penetrating networks, as another type of tangled motifs, are single nets that exhibit the peculiar feature of containing rings which pass through other components of the same network, and these rings must be topological shortest circuits of the net. To date, although considerable efforts have been directed to the construction of self-penetrating nets, only a limited number of cases are known.^{4–6} After all, the achievement of self-penetration continues to be a great challenge since it is comparatively difficult to predict the target compound prior to synthesis.^{5g}

In order to design such materials, control over the appropriate reaction conditions plays a key role in the synthetic procedure. The polymer topology strongly depends upon the chemical structure of ligands, the coordinative propensity of metal ions, solvent preference, and metal-to-ligand molar ratio, etc. While numerous organic molecules have been utilized as spacers, coordination polymers tuned by the coligands of carboxylates and N-donor molecules have witnessed an expansion development.⁷ As we found, those ligands bearing flexible lengths, charge-balance requirements, and different orientations of donor groups are likely to furnish advantages in the organization of

novel frameworks.^{8,9} One such ligand having O-donors with multiple coordination modes is 2,6-naphthalenedicarboxylic acid, a member of the polycarboxylates family.¹⁰ Furthermore, since those nonrigid ligands favor the fabrication of entangled motifs,^{6b,11,12a} a flexible long-chain imidazole-based 1,1'-(1,4-butanediyl)bis(imidazole) is combined with rigid or semirigid polycarboxylates to exploit 3-D self-penetrating networks.

On the other hand, lanthanide-transition-metal chemistry has been of great significance in the field of molecular magnetism. Particularly, 3d-4f cluster-based coordination polymers are expected to offer the possibility of single molecule magnet (SMM) in terms of the basic requirements such as high-spin ground-state and magnetic anisotropy. In the past, however, most research attention for the 3d-4f cluster complexes was primarily devoted to $\text{Gd}^{\text{III}}\text{--Cu}^{\text{II}}$ systems. As expected, Dy–Mn cluster-based complex seems to be an ideal choice for magnetic materials, and very few cases were reported to construct from such type of clusters, including $[\text{Mn}^{\text{III}}_{11}\text{Dy}^{\text{III}}_4]$, $[\text{Mn}^{\text{III}}_2\text{Dy}^{\text{III}}_2]$, $[\text{Mn}^{\text{III}}_4\text{Mn}^{\text{IV}}_2\text{Dy}^{\text{III}}_6]$ and $[\text{Mn}^{\text{III}}_6\text{Dy}^{\text{III}}_4]$.¹³

Although a variety of cluster-based SBUs have been established in various MOFs, the generation of high-connected topologies are extremely scarce as a result of the limited coordination number on transition metal centers.^{6d} Herein, we report in detail the synthesis and properties of two novel 3-D MOFs, $\text{Co}_3(\text{ndc})_3(\text{bbi})(\text{CH}_3\text{CN})_2$ (**1**) and $\text{Dy}_2\text{Mn}_3(\text{ndc})_6(\text{bipy})_2$ (**2**). Compound **1** contains an 8-connected topology, which, to the best of our knowledge, represents the highest connectivity net for self-penetration, equal to four others (with different topologies).⁶ Ferromagnetic material **2** exhibits an unprecedented 8-connected net with heteropentanuclear Dy_2Mn_3 clusters as 8-connected node.

Experimental Section

Materials and General Procedures. The reagents and solvents employed were commercially available and were used as received without further purification. Ligand bbi was synthesized as reported previously.¹⁴ The IR spectrum was recorded as KBr pellets on a Nicolet Magna-FT-IR 560 spectrometer in the 4000–400 cm^{-1} region. Elemental analysis for C, H, and N was performed on a Perkin-Elmer

* Corresponding author. Tel: +86-22-23508056. Fax: +86-22-23508056. E-mail: jmzheng@nankai.edu.cn.

[†] Nankai University.

[‡] Rutgers University.

[§] Monash University.

Table 1. Crystal Data and Structure Refinement for **1** and **2**

	1	2
formula	C ₅₀ H ₃₈ Co ₃ N ₆ O ₁₂	C ₉₂ H ₅₂ Dy ₂ Mn ₃ N ₄ O ₂₄
F _w	1091.65	2087.20
T [K]	298(2)	298(2)
crystal system	monoclinic	triclinic
space group	C2/c	P <bar{1}< td=""></bar{1}<>
a [Å]	18.379(4)	11.368(2)
b [Å]	13.593(3)	11.767(2)
c [Å]	18.835(4)	18.397(4)
α [deg]		104.96(3)
β [deg]	95.54(3)	97.18(3)
γ [deg]		112.78(3)
V [Å ³]	4683.8(16)	2121.0(7)
Z	4	1
d [g·cm ⁻³]	1.548	1.634
μ [mm ⁻¹]	1.122	2.254
Θ range [deg]	3.00–27.48	3.06–29.80
R ₁ and wR ₂ [<i>I</i> > 2σ(<i>I</i>)] ^a	0.0458, 0.1193	0.0580, 0.1244
R ₁ and wR ₂ (all data)	0.0599, 0.1270	0.0808, 0.1392

$$^a R_1 = \sum(|F_o - F_c|)/\sum|F_o|; wR_2 = [\sum w(F_o^2 - F_c^2)^2/\sum w(F_o^2)^2]^{1/2}.$$

240 analyzer. X-ray powder diffraction (XRPD) data were collected with a Rigaku D/max-RC diffractometer using a Cu target ($\lambda = 1.54060$ Å) operated at 50 kV and 180 mA. The thermogravimetric (TG) analysis was investigated on a standard TGA analyzer under nitrogen flow at a heating rate of 3 °C/min for all measurements. The magnetic measurements were performed on the Quantum Design SQUID MPMS XL-7 instruments. The diamagnetism of the sample and sample holder were taken into account.

Synthesis of Co₃(ndc)₃(bbi)(CH₃CN)₂ (1). A mixture of CoCl₂·6H₂O (0.24 g, 1.0 mmol), H₂ndc (0.22 g, 1.0 mmol) and bbi (0.06 g, 0.33 mmol) in the molar ratio of 3:3:1 was added into 6 mL of CH₃CN. Consequently, the resulting solution was transferred and sealed in a 25 mL Teflon-lined stainless steel vessel, which was heated at 140 °C for 60 h. After the reactor was slowly cooled to room temperature at a rate of 5 °C/h, pure purple block-shaped crystals were filtered off, and dried in air. Yield: 66% based on Co. Elemental analysis (%) calcd, C 55.01, H 3.51, N 7.70; found, C 55.03, H 3.55, N 7.72. IR (KBr): ν (cm⁻¹) = 2190 (s), 1613 (s), 1560 (s), 1496 (s), 1380 (vs), 776 (s), 704 (m), 663 (m).

Synthesis of Dy₂Mn₃(ndc)₆(bipy)₂ (2). A mixture of Dy₂O₃ (0.09 g, 0.25 mmol), MnCl₂·4H₂O (0.15 g, 0.75 mmol), H₂ndc (0.32 g, 1.5 mmol) and bipy (0.08 g, 0.50 mmol) in the molar ratio of 1:3:6:2 was dissolved in distilled water (6 mL). This solution was then adjusted to pH 2 with HNO₃. Consequently, the resulting solution was transferred and sealed in a 25 mL Teflon-lined stainless steel vessel, which was heated at 180 °C for three days. After the reactor was slowly cooled to room temperature at a rate of 5 °C/h, yellow block-shaped crystals were filtered off, washed with distilled water, and dried in air. Yield: 62% based on Dy. Elemental analysis (%) calcd, C 52.94, H 2.51, N 2.68; found, C 52.97, H 2.48, N 2.65. IR (KBr): ν (cm⁻¹) = 1602 (vs), 1556 (s), 1470 (m), 1385 (s), 795 (s), 737 (m), 714 (m).

X-ray Crystallographic Determinations. Single crystal analyses were performed on the RAXIS-RAPID AUTO CCD diffractometer systems (Mo K α radiation, $\lambda = 0.71073$ Å) for **1** and **2**. All data were collected for absorption by semiempirical method using the SADABS program. The program SAINT was applied for integration of the diffraction profiles.¹⁵ Data analyses were carried out with the program XPREP. The structures were solved with the direct method using SHELXS-97 followed by structure refinement on F^2 with the program SHELXL-97.¹⁶ All non-hydrogen atoms were refined anisotropically. Aromatic hydrogen atoms were assigned to calculated positions with isotropic thermal parameters. CCDC-642459 (**1**) and CCDC-672017 (**2**) contain the supplementary crystallographic data for this paper. These data can be obtained free of charge from The Cambridge Crystallographic Data Centre via www.ccdc.cam.ac.uk/data_request/cif. Crystal data and experimental details are summarized in Table 1.

Results and Discussion

Crystal Structure of **1.** Single crystal X-ray diffraction reveals that compound **1** crystallizes in the monoclinic space group C2/c, which is consistent with the XRPD experiment

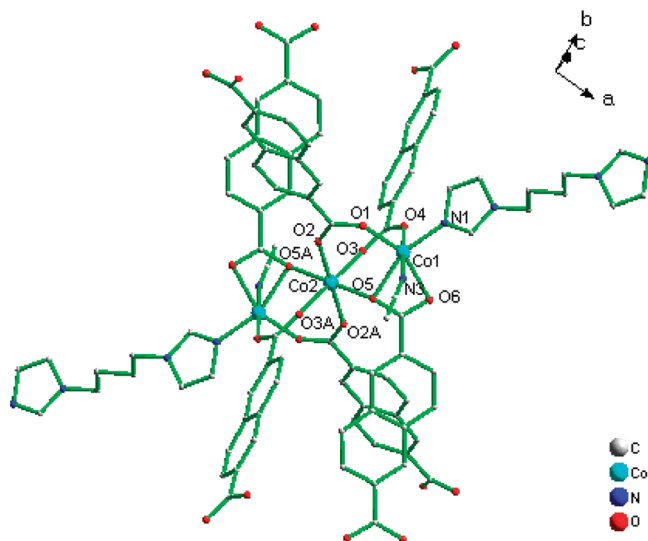


Figure 1. View of the local coordination environment for Co^{II} atom in **1**. Hydrogen atoms have been omitted for clarity. Note that the CH₃CN molecule is disordered over two positions; only one position is shown here.

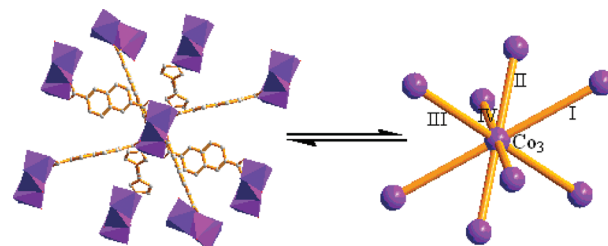


Figure 2. Perspective (left) and simplified (right) views of the 8-connected Co₃ core in **1**.

(Figure S1 in the Supporting Information). As shown in Figure 1, the fundamental building unit of polymer **1** contains one and a half unique Co^{II} ions, one and a half ndc²⁻ ions, half a bbi ligand and one coordinated CH₃CN molecule. Co1 is arranged in a distorted octahedral geometry, coordinated by four O_{carboxyl} atoms from three ndc²⁻ ions and two nitrogen atoms (one from bbi and the other from CH₃CN). Octahedral Co2 atom is bonded to six O_{carboxyl} atoms from six different ndc²⁻ ions (Co—O = 1.961(2)–2.214(2) Å). The Co2 atom is bridged to two neighboring Co1 by four —O—C—O— bridges and a pair of μ_2 —O_{carboxyl} atoms (O5 and O5A) to afford a Co₃ core. As shown in Figure 2, each Co₃ core is then connected to eight others through two bbi and six ndc²⁻ ions to generate a 3-D framework. Among the six ndc²⁻ linkers, two adopt the bidentate chelation mode (μ_4) and others with bidentate bridging mood (μ_4).

For **1**, one of the most prominent structural characteristics is the self-penetrating (Figure 3). By simplification of the structure of the Co₃(OCO)₆ species to an 8-connected node, the Schläfli topological description for **1** takes the form 4¹⁶·5⁸·6⁴. The topological index is computed via OLEX.¹⁷ As far as we know, no self-penetrated structure has been reported to contain nodes with connectivity higher than eight. Among those known 8-connected cases (4²⁴·5⁶, 4²⁰·6⁸, 4²¹·6⁷ and 4¹²·5⁶·6⁷·7²·8),⁶ all of them are based on bridged (4, 4) sheet as a subnet of the corresponding frameworks. In **1**, however, some 6-membered rings and two types of 4-membered rings are penetrated by the rods. Thus, the current architecture is topologically distinct from the reported 8-connected self-penetrating networks.

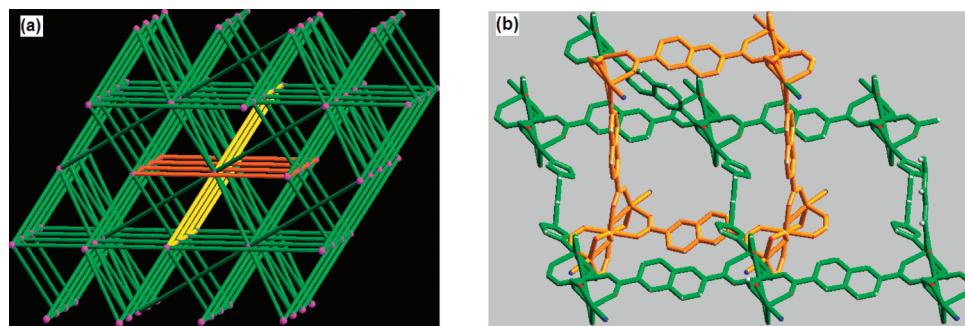


Figure 3. (a) Schematic representation of the 8-connected $4^{16} \cdot 5^8 \cdot 6^4$ self-penetrating nets and (b) local diagram of self-penetration in **1**.

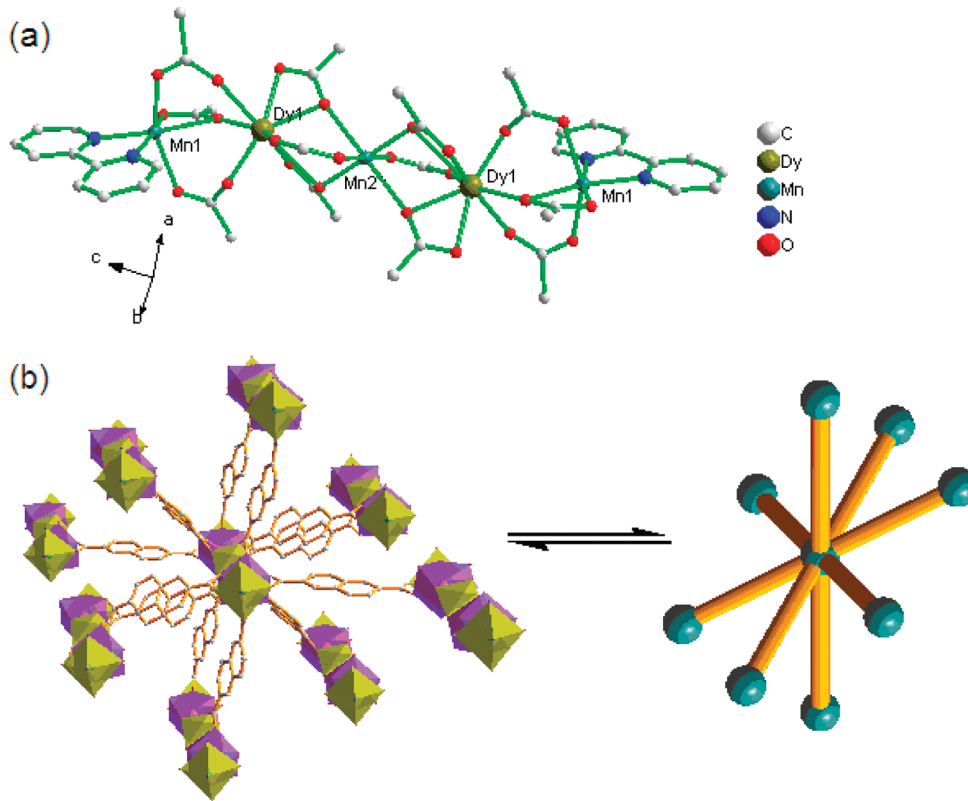


Figure 4. (a) Local coordination environment for Mn^{II} and Dy^{III} centers in **2**. Hydrogen atoms have been omitted for clarity; (b) perspective (left) and simplification (right) of the 8-connected heteropentanuclear core Dy_2Mn_3 .

Crystal Structure Description of **2.** The structure of **2** is composed of interconnected heteropentanuclear $\text{Dy}^{\text{III}}_2\text{Mn}^{\text{II}}_3$ units (Figure 4), which act as linear SBUs. In this SBU, there exist one and a half crystallographically unique Mn^{II} and one Dy^{III} ion. Each Mn^{II} atom (two symmetry-equivalent Mn1 and one Mn2) is six-coordinate to form octahedral geometry. Four oxygen atoms deriving from three carboxyl groups occupy the four coordination sites of Mn1, and the remaining two sites are chelated to two nitrogen atoms from bipy. Mn2 is surrounded by six oxygen atoms from six different ndc²⁻ ions. The average Mn–O separation ranges from 2.069(5) to 2.508(4) Å. The two symmetry-related Dy^{III} ions show a typical eight-coordinate environment, which is filled with eight oxygens from six carboxylates (Dy–O = 2.198(4)–2.780(5) Å). Dy^{III} is related to Mn1 and Mn2 via one O atom in corner-sharing mode and two O atoms in edge-sharing mode, respectively, leading to a $\text{Dy}^{\text{III}}_2\text{Mn}^{\text{II}}_3$ cluster SBU. Each $\text{Dy}^{\text{III}}_2\text{Mn}^{\text{II}}_3$ SBU then bridges eight other SBUs by twelve bridging ndc²⁻ ligands to afford an overall 3-D MOF (Figure 5a).

More significantly, polymer **2** represents the first $\text{Dy}^{\text{III}}_2\text{Mn}^{\text{II}}_3$ (3d-4f) heteropentanuclear complex. We notice this structure is totally different from the reported Gd_2Mn_3 complex which is composed of discrete $\text{Gd}_2\text{Mn}_3(\text{CH}_2\text{C}(\text{CH}_3)\text{COO})_{12}(\text{bipy})_2$ molecules.¹⁸ Topological study suggests this compound falls into an 8-connected network with $3^6 \cdot 4^{18} \cdot 5^3 \cdot 6$ topology as long as $\text{Dy}^{\text{III}}_2\text{Mn}^{\text{II}}_3$ cluster-based SBU is treated as an 8-connected node (Figure 5b), and only two cases have been found with this topological notation.¹⁹ Based on the assignment of clusters, compound **2** would be described as hexagonal primitive lattice: the parallel hexagonal (3, 6) sheets are aligned perpendicular to the diagonal [1, 1, 1]. Obviously, the topology of polymer **2** distinguish from the commonly encountered body-centered-cubic (bcc) lattice in which the parallel (4, 4) sheets are cross-linked by zigzag chains.

Magnetic Property of **1.** Temperature-dependent magnetic susceptibility for **1** was measured in the temperature range of 2–300 K. The molar magnetic susceptibility higher than 30 K follows the Curie–Weiss law with $C = 7.00 \text{ cm}^3 \text{ K mol}^{-1}$, and

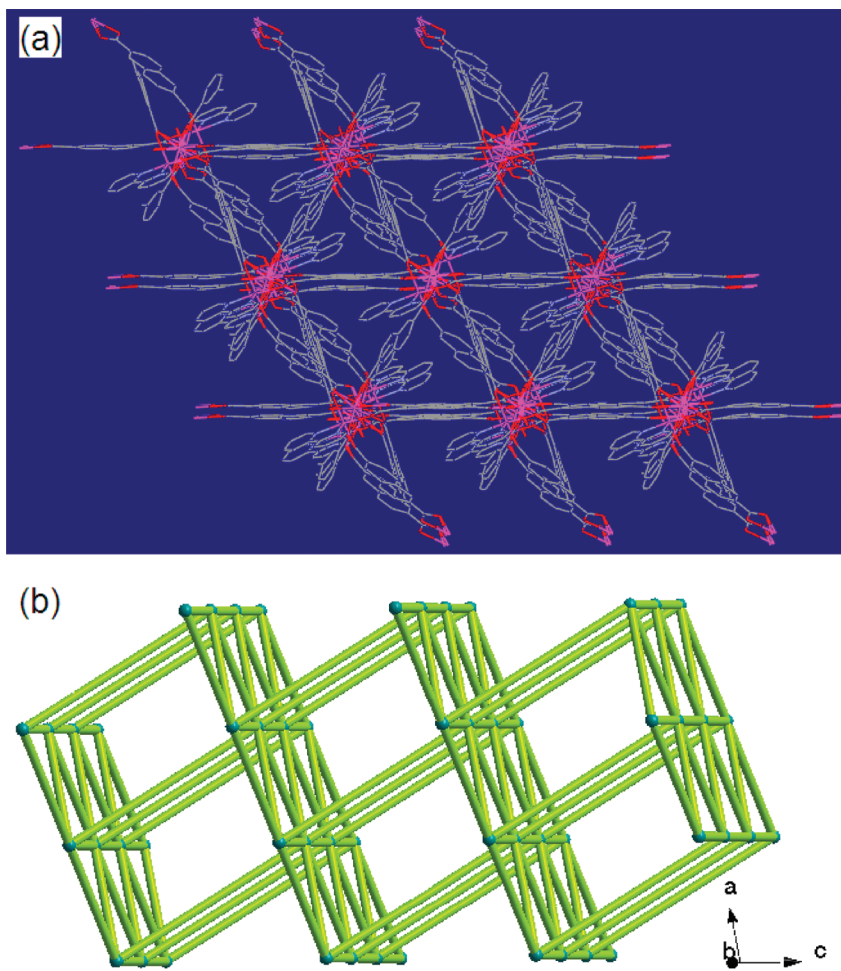


Figure 5. (a) 3-D supramolecular motif; (b) schematic representation of the 8-connected $3^6 \cdot 4^{18} \cdot 5^3 \cdot 6$ topological network in **2**.

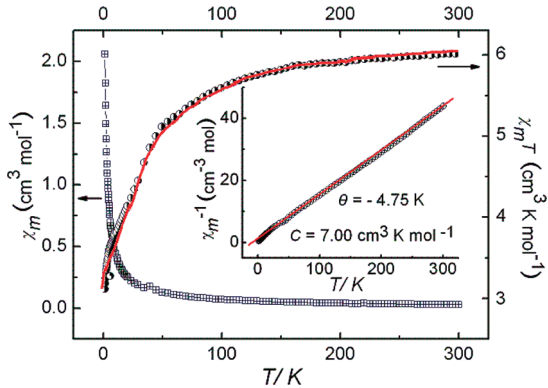


Figure 6. Plot of χ_m and $\chi_m T$ versus T for **1**. The field strength used was $H = 500$ Oe. Inset: χ_m^{-1} versus T . The red line represents the best fit.

a negative $\theta = -4.75$ K, which suggests the antiferromagnetic interactions within the trimeric Co_3 core are operative. The $\chi_m T$ product (Figure 6) for each Co_3 core of $6.02 \text{ cm}^3 \text{ K mol}^{-1}$ at room temperature is larger than that expected ($5.63 \text{ cm}^3 \text{ K mol}^{-1}$) for three magnetically uncoupled Co^{II} ($S = 3/2$). The variation of the value $\chi_m T$ as a function of temperature shows a continuous decrease with T between 300 and 2 K ($3.25 \text{ cm}^3 \text{ K mol}^{-1}$) in agreement with the negative Weiss temperature. These features confirm the existence of antiferromagnetic interactions and the effect of spin-orbit coupling known for octahedral Co ions.²⁰

Previously, we have appropriately fitted the magnetic data for Co_3 cluster,^{12b} which indicates it is necessary to introduce some additional magnetic parameters. Similarly, the data of **1** could be simulated using the HDVV (Heisenberg–Dirac–Van Vleck) isotropic spin Hamiltonian $H = -2J S_1 S_2$, and the magnetic interaction between two terminal Co^{II} atoms should be omitted. The best-fit parameters are listed as follows: $J = -6.87 \text{ cm}^{-1}$, $g = 2.21$, $\chi_{\text{TIP}} = 380 \times 10^{-6} \text{ cm}^3 \text{ mol}^{-1}$, $\rho = 0.009$ and $R = 2.33 \times 10^{-4}$, where the term χ_{TIP} is the temperature-dependent paramagnetic contribution and ρ represents the possible paramagnetic impurity of the sample.

Magnetic Property of 2. Variable-temperature magnetization measurement of **2** was performed in the 2–300 K range at 500 Oe applied field. The temperature dependence of the reciprocal susceptibility (χ_m^{-1}) above 2 K obeys the Curie–Weiss law ($\chi_m = C/(T - \theta)$) with Curie constant $C = 42.3 \text{ cm}^3 \text{ K mol}^{-1}$ and a Weiss constant $\theta = +1.97$ K, thus indicating a ferromagnetic coupling interaction between the Dy^{III} and Mn^{II} ions (inset of Figure 7b). The $\chi_m T$ value of $41.54 \text{ cm}^3 \text{ K mol}^{-1}$ is very close to that of $41.47 \text{ cm}^3 \text{ K mol}^{-1}$ expected for three magnetically isolated high-spin Mn^{II} ($13.13 \text{ cm}^3 \text{ K mol}^{-1}$) plus two Dy^{III} ions ($28.34 \text{ cm}^3 \text{ K mol}^{-1}$) in a $\text{H}_{15/2}$ ground state ($g = 4/3$; $J = 5/2$, $L = 5$, $J = 15/2$). As shown in Figure 7a, the monotonic increase in $\chi_m T$ until a maximum ($47.13 \text{ cm}^3 \text{ K mol}^{-1}$) at $T_{\max} = 37.5$ K with cooling temperature is also characteristic of ferromagnetic exchange. Upon further lowering the temperature to 2 K, the product $\chi_m T$ abruptly decreases to a minimum ($36.88 \text{ cm}^3 \text{ K mol}^{-1}$), which is probably due to the saturation effect.

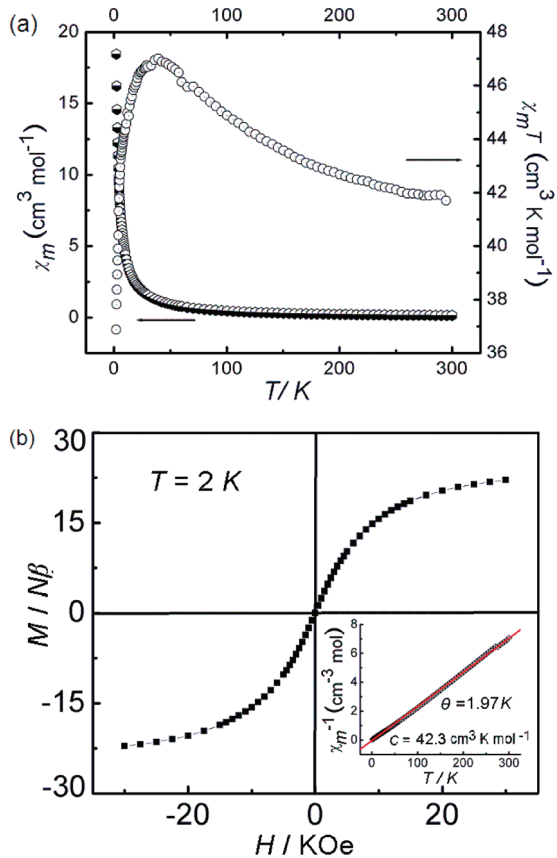


Figure 7. (a) Plot of χ_m and $\chi_m T$ versus T for **2** at $H = 500$ Oe; (b) the hysteresis loop for **2** at 2 K. Inset: χ_m^{-1} versus T . The red line represents the best fit.

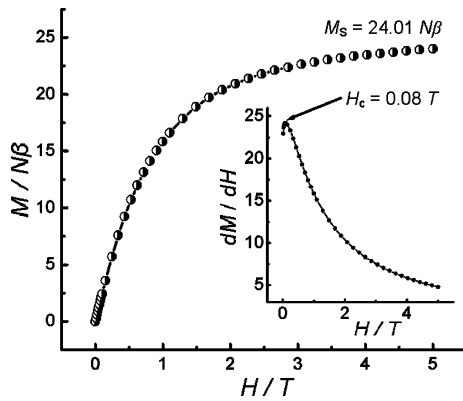


Figure 8. Plot of field-dependent magnetization for **2** at 2 K. The inset shows the critical field H_c .

Further magnetic characterization of **2** was performed by field-dependent magnetization at $T = 2$ K. Figure 8 shows the isotherm magnetization experiences a rapid increase in $M - H$ at the start of lower field, followed by a smooth increase to the saturation magnetization at $H = 5$ T. The $M_s = 24.01 N\beta$ for each $Dy^{III}_2Mn^{II}_3$ unit is much less than the theoretical value. The critical field $H_c = 800$ Oe is approximately detected by the sharp peak of dM/dH vs H (inset of Figure 8). A sigmoidal-shaped hysteresis loop is provided in Figure 7, indicating the soft ferromagnetic behavior because of nondetectable coercivity in **2**.

Thermal stabilities by TG. Figure S2 in the Supporting Information displays the first weight loss (calcd, 10.1%; found, 9.7%) in **1** at about 95 °C corresponding to the coordination CH_3CN molecules, which is followed by a

strong exothermic peak at 275 °C where the decomposition of the host framework of **1** starts. The resulting product should be CoO (calcd, 20.5%; found, 20.7%). Polymer **2** remains stable up to *ca.* 438 °C. A strong exothermic peak occurs at 520 °C, indicating the complete cleavage of the integrated skeleton. The remaining residue is presumed to be Dy_2O_3 and MnO (calcd, 28.1%; found, 28.9%).

Conclusions

In summary, we have successfully developed a rational synthetic strategy for desired architectures causing the construction of two interesting MOFs composed of cluster-based SBUs. Toward this effort, a novel 8-connected networks with $4^{16} \cdot 5^8 \cdot 6^4$ topology is presented for the first time which equals the highest connectivity for monometallic self-penetrating networks. We have also established an unprecedented heteropentanuclear $Dy^{III} - Mn^{II}$ system, showing highly 8-connected $3^6 \cdot 4^{18} \cdot 5^3 \cdot 6$ networks with the treatment of cluster-based Dy_2Mn_3 SBU as a node in which soft ferromagnetic behavior is confirmed. Such investigations demonstrate the utility of current methodology and versatility of rigid H_2NDC for the high-dimensional supramolecules. As a result of the above impetus, continuous attempts are underway to prepare novel coordination polymers with unique attributes and desirable applications.

Acknowledgment. This work was supported by the National Natural Science Foundation of China for financial support (50872057).

Supporting Information Available: XRPD patterns; TG curves. This material is available free of charge via the Internet at <http://pubs.acs.org>.

References

- (a) Bourne, S. A.; Moulton, J.; Lu, B.; Zaworotko, M. *J. Chem. Commun.* **2001**, 861. (b) Li, Y. H.; Su, C. Y.; Goforth, A. M.; Shimizu, K. D.; Gray, K. D.; Smith, M. D.; zur Loye, H. C. *Chem. Commun.* **2003**, 1630. (c) Carlucci, L.; Ciani, G.; Moret, M.; Proserpio, D. M.; Rizzato, S. *Angew. Chem., Int. Ed.* **2000**, 39, 1506.
- (a) Miller, J. S. *Adv. Mater.* **2001**, *13*, 525. (b) Kitaura, R.; Seki, K.; Akiyama, G.; Kitagawa, S. *Angew. Chem., Int. Ed.* **2003**, *42*, 428.
- (a) Batten, S. R.; Robson, R. *Angew. Chem., Int. Ed.* **1998**, *37*, 1460. (b) Carlucci, L.; Ciani, G.; Proserpio, D. M. *Coord. Chem. Rev.* **2003**, *247*, 246. (c) Batten, S. R. *CrystEngComm* **2001**, *3*, 67. (d) Blatov, V. A.; Carlucci, L.; Ciani, G.; Proserpio, D. M. *CrystEngComm* **2004**, *6*, 377.
- (a) Wang, X. L.; Qin, C.; Wang, E. B.; Li, Y. G.; Su, Z. M.; Xu, L.; Carlucci, L. *Angew. Chem., Int. Ed.* **2005**, *44*, 5824. (b) Long, D. L.; Hill, R. J.; Blake, A. J.; Champness, N. R.; Hubberstey, P.; Wilson, C.; Schröder, M. *Chem.—Eur. J.* **2005**, *11*, 1384.
- (a) Tong, M. L.; Chen, X. M.; Batten, S. R. *J. Am. Chem. Soc.* **2003**, *125*, 16170. (b) Zhan, S. Z.; Li, D.; Zhou, X. P.; Zhou, X. H. *Inorg. Chem.* **2006**, *45*, 9163. (c) Huang, X. H.; Sheng, T. L.; Xiang, S. C.; Fu, R. B.; Hu, S. M.; Li, Y. M.; Wu, X. T. *Inorg. Chem.* **2007**, *46*, 497. (d) Bi, M. H.; Li, G. H.; Zou, Y. C.; Shi, Z.; Feng, S. H. *Inorg. Chem.* **2007**, *46*, 604. (e) Zhang, S. S.; Zhan, S. Z.; Li, M.; Peng, R.; Li, D. *Inorg. Chem.* **2007**, *46*, 4365. (f) Zhai, Q. G.; Lu, C. Z.; Chen, S. M.; Xu, X. J.; Yang, W. B. *Cryst Growth Des.* **2006**, *6*, 1393. (g) Yang, J.; Ma, J. F.; Liu, Y. Y.; Batten, S. R. *CrystEngComm* **2009**, *11*, 151.
- (a) Wang, X. L.; Qin, C.; Wang, E. B.; Su, Z. M.; Xu, L.; Batten, S. R. *Chem. Commun.* **2005**, 4789. (b) Wang, X. L.; Qin, C.; Wang, E. B.; Su, Z. M. *Chem.—Eur. J.* **2006**, *12*, 2680. (c) Xiao, D. R.; Li, Y. G.; Wang, E. B.; Fan, L. L.; An, H. Y.; Su, Z. M.; Xu, L. *Inorg. Chem.* **2007**, *46*, 4158. (d) Li, Z. G.; Wang, G. H.; Jia, H. Q.; Hu, N. H.; Xu, J. W.; Batten, S. R. *CrystEngComm* **2008**, *10*, 983.
- (a) Lu, J. Y. *Coord. Chem. Rev.* **2003**, *241*, 327. (b) James, S. L. *Chem. Soc. Rev.* **2003**, *32*, 276. (c) Moulton, B.; Zaworotko, M. *J. Chem. Rev.* **2001**, *101*, 1629.

- (8) (a) Suh, M. P.; Moon, H. R.; Lee, E. Y.; Jang, S. Y. *J. Am. Chem. Soc.* **2006**, *128*, 4710. (b) Zang, S. Q.; Su, Y.; Li, Y. Z.; Ni, Z. P.; Zhu, H. Z.; Meng, Q. *J. Inorg. Chem.* **2006**, *45*, 3855. (c) Zang, S. Q.; Su, Y.; Duan, C. Y.; Li, Y. Z.; Zhu, H. Z.; Meng, Q. *J. Chem. Commun.* **2006**, 4997.
- (9) (a) Chen, B.; Ockwig, N. W.; Millward, A. R.; Contreras, D. S.; Yaghi, O. M. *Angew. Chem., Int. Ed.* **2005**, *44*, 4745. (b) Lin, X.; Jia, J.; Zhao, X.; Thomas, K. M.; Blake, A. J.; Walker, G. S.; Champness, N. R.; Hubberstey, P.; Schröder, M. *Angew. Chem., Int. Ed.* **2006**, *45*, 7358. (c) Chen, B.; Ockwig, N. W.; Fronczek, F. R.; Contreras, D. S.; Yaghi, O. M. *Inorg. Chem.* **2005**, *44*, 181.
- (10) (a) Choi, E. Y.; Park, K.; Yang, C. M.; Kim, H.; Son, J. H.; Lee, S. W.; Lee, Y. H.; Min, D.; Kwon, Y. U. *Chem.—Eur. J.* **2004**, *10*, 5535. (b) Chun, H.; Dybtsev, D. N.; Kim, H.; Kim, K. *Chem.—Eur. J.* **2005**, *11*, 3521. (c) Dincă, M.; Long, J. R. *J. Am. Chem. Soc.* **2005**, *127*, 9376.
- (11) (a) Wen, L. L.; Dang, D. B.; Duan, C. Y.; Li, Y. Z.; Tian, Z. F.; Meng, Q. *J. Inorg. Chem.* **2005**, *44*, 7161. (b) Song, L.; Li, J. R.; Lin, P.; Li, Z. H.; Li, T.; Du, S. W.; Wu, X. T. *Inorg. Chem.* **2006**, *45*, 10155.
- (12) (a) Chen, P. K.; Che, Y. X.; Xue, L.; Zheng, J. M. *Cryst. Growth Des.* **2006**, *6*, 2517. (b) Chen, P. K.; Che, Y. X.; Zheng, J. M.; Batten, S. R. *Chem. Mater.* **2007**, *19*, 2162.
- (13) (a) Mishra, A.; Wernsdorfer, W.; Abboud, K. A.; Christou, G. *J. Am. Chem. Soc.* **2004**, *126*, 15648. (b) Mishra, A.; Wernsdorfer, W.; Parsons, S.; Christou, G.; Brechin, F. K. *Chem. Commun.* **2005**, 2086. (c) Zaleski, C. M.; Depperman, E. C.; Kampf, J. W.; Kirk, M. L.; Pecoraro, V. L. *Angew. Chem., Int. Ed.* **2004**, *43*, 3912. (d) Zaleski, C. M.; Kampf, J. W.; Mallah, T.; Kirk, M. L.; Pecoraro, V. L. *Inorg. Chem.* **2007**, *46*, 1954.
- (14) Ma, J. F.; Yang, J.; Zheng, G. L.; Li, L.; Liu, J. F. *Inorg. Chem.* **2003**, *42*, 7531.
- (15) Bruker A. X. S. *SAINT Software Reference Manual*: Bruker Analytical X-ray Instruments, Inc., Madison, WI, 1998.
- (16) Sheldrick, G. M. *SHELXTLNT Version 5.1, Program for Solution and Refinement of Crystal Structures*; University of Göttingen: Germany, 1997.
- (17) Dolomanov, O. V.; Blake, A. J.; Champness, N. R.; Schröder, M. *J. Appl. Crystallogr.* **2003**, *36*, 1283.
- (18) Wu, B. *Dalton Trans.* **2006**, 5113.
- (19) Qi, Y.; Che, Y. X.; Zheng, J. M. *CrystEngComm* **2008**, *10*, 1137, and references cited therein.
- (20) Yang, J.; Yue, Q.; Li, G. D.; Cao, J. J.; Li, G. H.; Chen, J. S. *Inorg. Chem.* **2006**, *45*, 2857.

CG8013893